Supplementary Information

Designing an Ordered Template of Cylindrical Arrays based on a Simple Flat Plate Confinement of Block Copolymers: A Coarse-Grained Molecular Dynamics Study

Shubham Pinge[1], Guanyang Lin[2], Durairaj Baskaran[2], Munirathna Padmanaban[2], and Yong Lak Joo[1,*]
[1]Robert Frederick Smith School of Chemical and Biomolecular Engineering, Cornell University, Ithaca, NY 14853 (USA)
[2]R&D Center, EMD Performance Materials Corp., 70 Meister Avenue, Somerville, NJ 08876, USA

1. Estimation of the Flory-Huggins parameter

The following linear expression has been derived by Horsch et[1] al to relate χN with the polymer MD parameters:

$$\chi N = \left[\frac{(9.48 \pm 0.11)\varepsilon}{k_B T} - 0.09\right] N \quad \text{- (1)}$$

The author further considers the Ginsburg parameter to calculate the effective polymer chain length.

$$\bar{N} = 6^3 (R_g^3 \rho)^2 \quad \text{- (2)}$$

Where R_g is the BCP radius of gyration and ρ = polymer site density = $0.85\sigma^{-3}$

For a finite sized polymer chain, the effective polymer chain length for weak coupling is shown in the publication by Groot and Madden[2] to be:

$$(\chi N)_{eff} = \frac{\chi N}{1 + 3.9 N^{-1/3}} \quad \text{- (3)}$$

SCFT assumes the ideal R_g scaling of 0.5 for the Flory-Huggins parameter estimation. Horsch et al finds that the R_g scales as $v = 0.69$ for their chain lengths $5 \leq N \leq 10$

For the longer chains employed in this study the scaling exponent $v = 0.63$ seems to be a better fit as evident from Figure S1a-b. Combining the equations 1, 2 and 3 for the scaling exponent $v = 0.69$, we get equation 4 that is used to estimate the Flory-Huggins parameter.

$$(\chi N)_{eff} \approx \frac{\left[(9.48 \pm 0.11)^{\varepsilon}/_{kT} - 0.09\right]N}{1 + 3.9N^{-0.59}} \quad \text{- (4)}$$

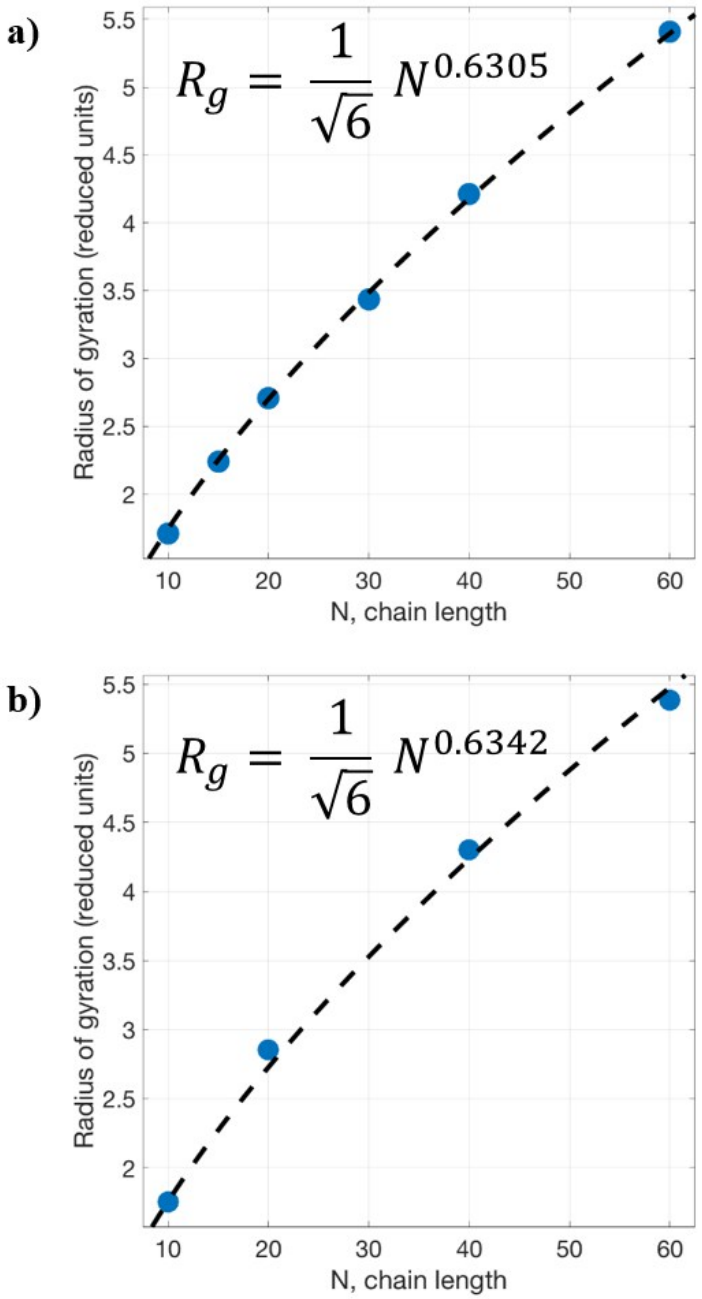

Figure S1:Radius of gyration scaling for a) volume fraction = 0.3 and b) volume fraction = 0.5

2. BCP domain length scaling

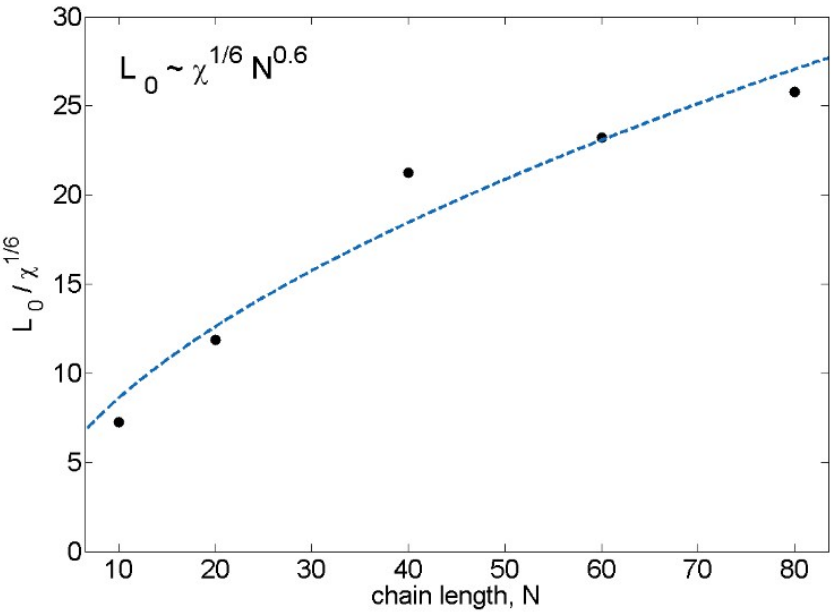

Figure S2: Scaling for BCP domain length, Lo as a function of the BCP chain length, *N*. The minor phase volume fraction is perforated lamellae.

Bulk trials as described in the previous section were carried out for volume fraction 0.3. The morphology formed is perforated lamellae. The BCP domain length is measured for chain lengths: *N*10, *N*20, *N*40, *N*60 and *N*80. *N*120 required a substantially large simulation box size which would be computationally difficult. Hence a scaling of $\boldsymbol{L_0 \sim \chi^{1/6} N^{0.6}}$ was used to predict L_0 for *N*120 used in table 3 (page 16, main paper)

3. Flat plate trials at 17 σ, minor phase volume fraction = 0.35

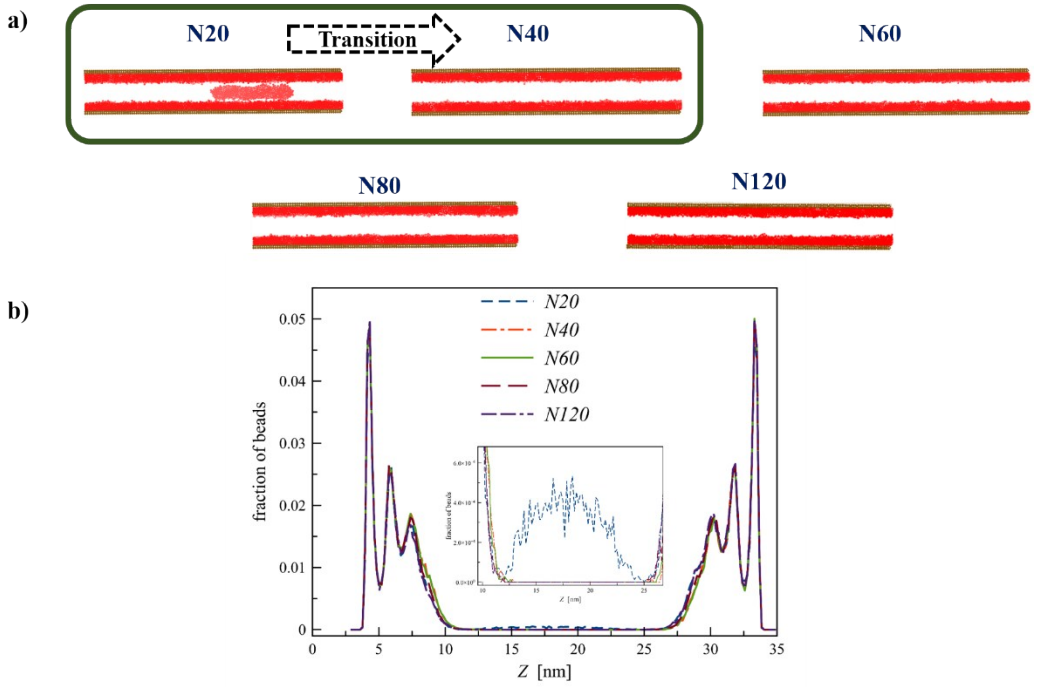

Figure S3: Morphology formed for flat plate – 17 σ confinement trials at minor phase volume fraction of 0.35. b) Concentration plots for a).
Note: Only minor phase of the BCP is seen, major phase has been hidden for clarity in a)

If we increase the volume fractions to 0.35 for the 17 σ flat plate trials, the transition from the continuous three-domain sandwich to a two-domain structure also occurs at *N*20-*N*40, but the middle minor phase domain for *N*20 has a much lower concentration as compared to the lower volume fraction trials. This can be attributed to the poor screening caused by the major phase domains for the higher minor phase volume fraction trials. As these trials have a lower major phase concentration, the effective screening effect caused by the major phase shielding the bulk minor phase domains from the surface domains is lower. Hence the middle domains get redistributed among the two surface domains leading to the observed geometry.

4. Design plot generation for different BCP minor-phase volume fraction

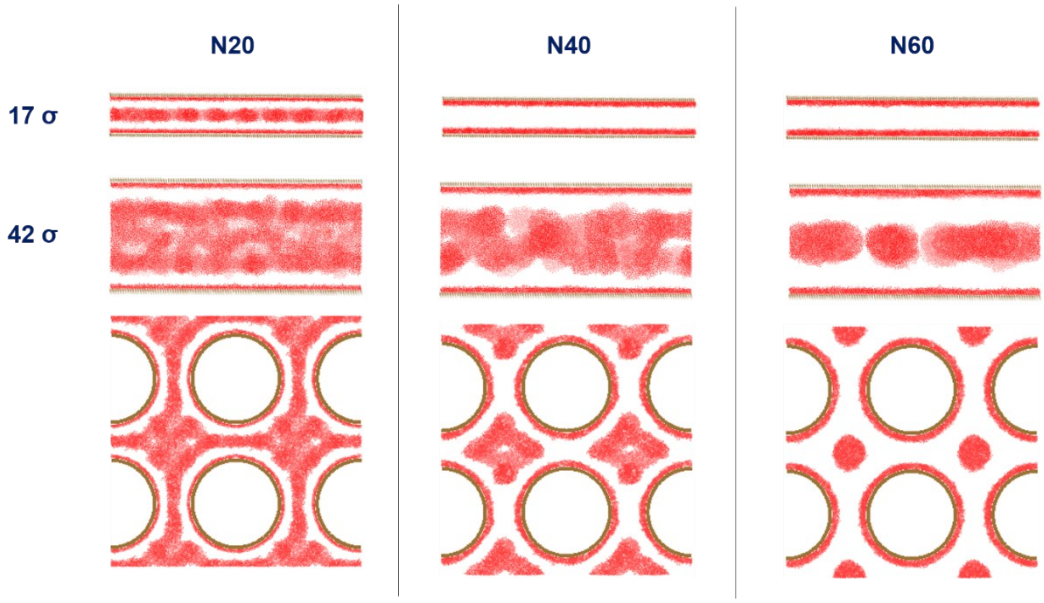

Figure S4: Comparison of the morphologies formed by the flat plate geometries at two confinements -17 σ and 42 σ with the cubically packed cylinder template at volume fraction-0.25

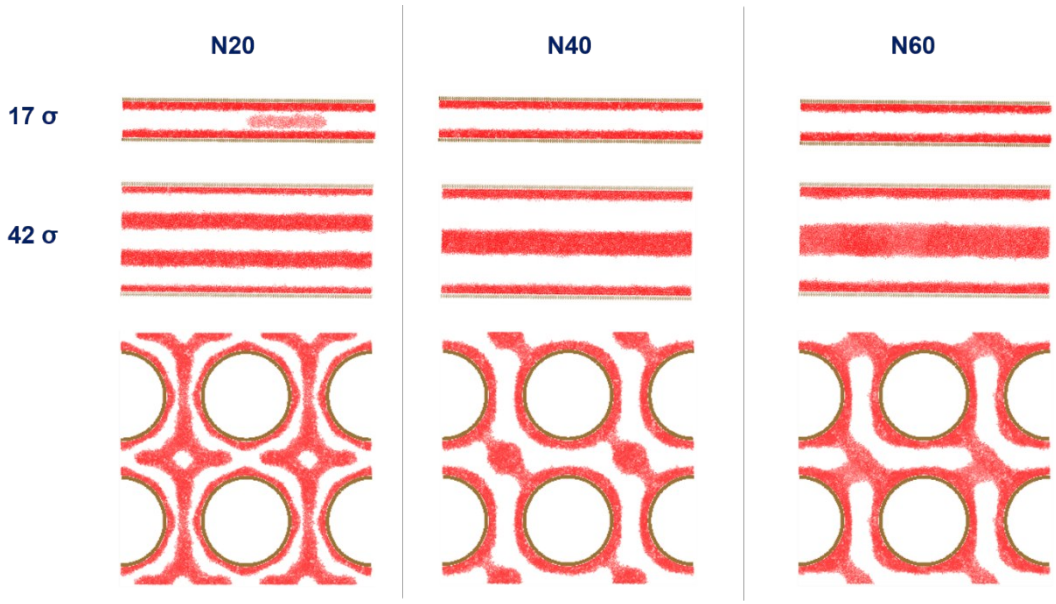

Figure S5: Comparison of the morphologies formed by the flat plate geometries at two confinements -17 σ and 42 σ with the cubically packed cylinder template at volume fraction-0.35

As seen in the results section of the main paper, there is a strong correlation between the flat plate studies at two confinement lengths (*17σ* and *42σ* separations). The results were performed at the default minor phase volume fraction of 0.30. The trials were then reproduced at two other volume fractions of 0.25 and 0.35 . Figure S3 for volume fraction 0.25 shows a strong correlation similar to the default volume fractions. *N20* formed a three-domain morphology for the lower confinement length and a five domain structure with heavy micro-bridging among the domains for the higher confinement. This observation is also seen in the two regions of interests of maximum and minimum confinement length for the ordered cylinder template. The correlation also holds true for *N40* and *N60* with the *N60* forming cubically packed cylinders.

For the higher volume fraction of 0.35, *N20* shows a strong correlation among the flat plate and cubically packed cylinders with the minimum confinement length showing a two domain with a minuscule blob while the maximum confinement length forming a four domain morphology. The ordered pillars template also shows same number of continuous domains in the two regions of interest. Increasing the molecular weight also shows a similarity between the two types of geometric templates but the correlation is not as strong due to the micro-bridging observed. The micro-bridging is caused due to increased minor phase concentration in the system.

Effect of increasing the pillar height for ordered pillars template: The trials in the main paper have shown that under favorable conditions, the cubically packed silica pillars can direct the BCP to form minor phase cylinders that are also cubically packed. As these cylinders serve as a pathway for the transport of electrons, uniformity along the pillar height is desired. For some applications, longer channels may be desired for the flow of electrons. Trials have thus been performed using a similar template, but with taller pillars. The new pillar height has been increased from 62.107 σ

(111.79nm) to 100 σ (180nm) keeping the *x y* dimensions of the box and polymer properties unchanged. The increase in height also leads to more number of BCPs in the system, further surging the computational expense of the simulations.

Trends similar to the default pillar height trials were seen in the thickness of the minor phase on the surfaces and the qualitative nature of the morphology formed for the new pillar height trials. The main distinction for the two trials arises in the inability of the cylinders formed by the taller pillars to maintain uniformity in *z*. While *N40* trials under default settings formed uniform cylinders (Figure 6, main paper), these trials show complete cylinder formation but with some loss in the *z* orientation. Large simulations are expected to show lesser uniformity as the polymers find it difficult to maintain the orientation throughout the limits of the *z* direction. Some other distinction in the new trials are for *N20*. Just as in the default pillar height case, *N20* forms curved perforated lamellae morphology, but the lamellae show sharp edges as opposed to the smoother structures formed for the default case. This loss in curvature can be attributed to the inability of the minor phase to lie in the same constricted lamellae area in the bulk of the template across the pillar height. *N60* trials form cubically packed cylinder with slight micro-bridging similar to its default counterpart. These cylinders are incompletely formed with scarcity of minor phase beads in many areas across the pillar height.

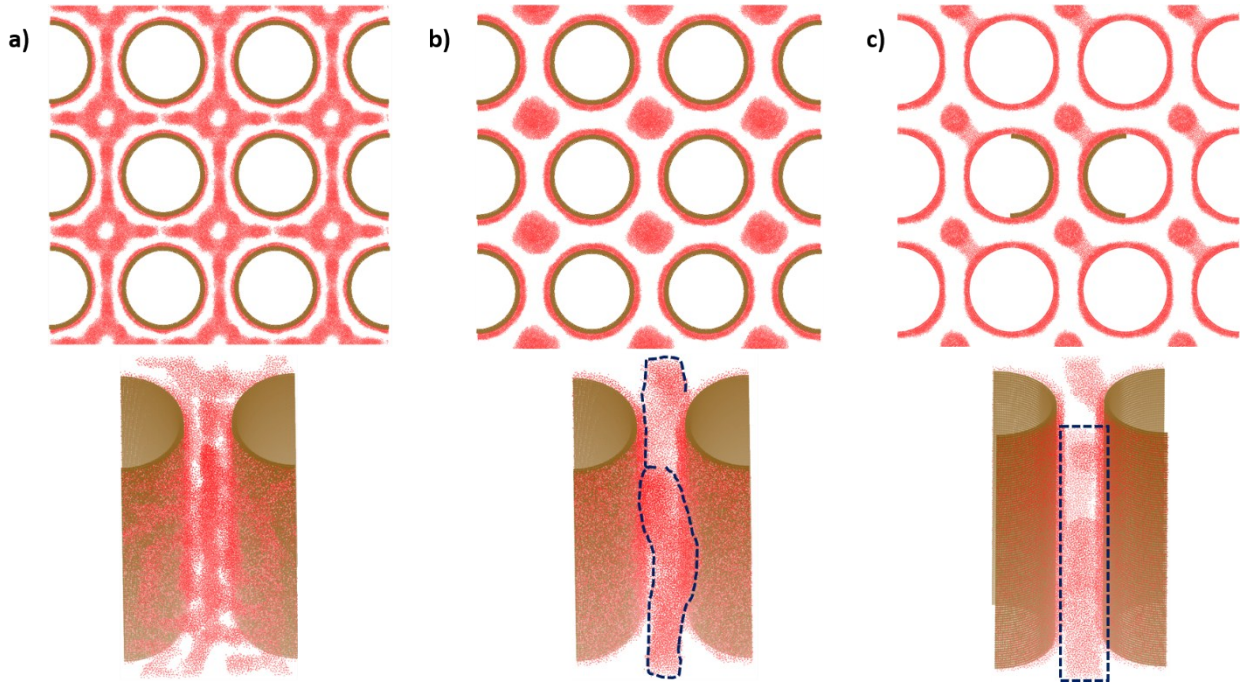

Figure S6: Morphology formed by taller pillars for BCP volume fraction 0.3 at three different chain lengths a) *N20* b) *N40* and c) *N60*. Minor phase is seen in red and major phase is hidden.

References:

1. Horsch MA, Zhang Z, Iacovella CR, Glotzer SC. Hydrodynamics and microphase ordering in block copolymers: Are hydrodynamics required for ordered phases with periodicity in more than one dimension?. The Journal of chemical physics. 2004 Dec 8;121(22):11455-62.
2. Groot RD, Madden TJ. Dynamic simulation of diblock copolymer microphase separation. The Journal of chemical physics. 1998 May 22;108(20):8713-24.